Tuning supramolecular chirality in *nano* and mesoscopic porphyrin J-aggregates

Roberto Zagami,[‡] Maria A. Castriciano,[‡] Andrea Romeo,[‡,†] * Mariachiara Trapani,[‡] Rolando Pedicini,[#] Luigi Monsù Scolaro[‡,†].*

[‡] CNR-ISMN, Istituto per lo Studio dei Materiali Nanostrutturati, c/o Dipartimento di Scienze Chimiche, Biologiche, Farmaceutiche ad Ambientali 98166, V.le F. Stagno D'Alcontres 31 Messina, Italy. E-mail: castriciano@pa.ismn.cnr.it

[†] Dipartimento di Scienze Chimiche, Biologiche, Farmaceutiche ad Ambientali, and C.I.R.C.M.S.B., University of Messina, V.le F. Stagno D'Alcontres 31, Vill. S. Agata, 98166 Messina, Italy. E-mail: anromeo@unime.it

[#] CNR-ITAE Istituto di Tecnologie Avanzate per l'Energia, Via Salita Santa Lucia Sopra Contesse 5, 98126, Messina, Italy

KEYWORDS

Nanoaggregates, mesoscopic, porphyrin, chirality, disassembling.

ABSTRACT

In natural light-harvesting systems, chirality represents a crucial point being one of the recurrent motifs. The ability to tune supramolecular chirality both on nano and meso scale is a key topic on the design of mimetic antenna systems. Here we describe a non-covalent approach to achieve mesoscopic clusters, based on spermine and the diacid form of $TPPS_4$ porphyrin, having a sea urchin-like morphology, whose chirality can be induced by the presence of L- or D-tartrate under mild acidic conditions. The mechanism proposed for the formation of these clusters deals wiht the formation of peculiar optically active J-nanoaggregates, which serve as nuclei for further growth into mesoscopic structures. Poly(vinylsulfonate) has been used to scavenge the polyamine and thereby foster disaggregation. The kinetics of this process show a biphasic behavior characterized by a rapid removal of spermine externally bound to porphyrin monomeric units followed by a stripping-out of the polyamine which is tightly bound to the J-nanoaggregates. A careful choice of experimental conditions allows precise control of the disaggregation kinetics, leading to the isolation of J-nanoaggregates. These latter species exhibit chirality even in the absence of a chiral inducer. This feature, together with the anomalous behavior of the CD signal of the mesoscopic aggregates containing optically active tartrate, have been explained in terms of screening hypochromism, differential scattering and structural rearrangements.

INTRODUCTION

Supramolecular aggregates of porphyrins and related macrocycles have been extensively investigated due to their similarity to biologically-relevant light harvesting antennas. [1,2] In particular, the so-called porphyrin “J-aggregates” have attracted a large interest. [3-18] These latter are molecular

dyes aggregates noteworthy in displaying both a very intense and narrow absorption peak, namely known as a J-band, largely red-shifted with respect to monomer absorption. An intriguing property of these supramolecular assemblies of achiral monomers is the appearance of chirality induced by chiral biases such as: i) chiral templating agents [8, 19, 20], ii) vortex motion, [21, 22] iii) stirring, [22, 23, 24, 25-27] iv) application of rotational, gravitational and orienting forces [28] and v) weak thermal forces acting as an asymmetrical physical perturbation.[29] Tetra-anionic *meso*-tetrakis(4-sulfonatophenyl)porphyrin ($TPPS_4$) has been most extensively explored, and has been proved to form such J-aggregates consequent to acidification and/or by the interaction with cationic species. [3, 5, 15, 17, 30, 31, 32, 33] A series of studies have demonstrated the presence in solution of assemblies whose size ranges from nano up to the micrometer scale. [31, 16, 17] Various spatial arrangements have been proposed, although most evidence points to a nanotube-like structure. [30, 34-36, 37-39] A transition between rod-like and fractal structures has also been proved, emphasizing a structure-dependent optical activity induced by a chiral template, thus raising an intriguing question about transmission of chirality from a local or molecular level up to the mesoscopic regime.[31] When spermine is used as a cationic template, features of these fractal structures include a large enhancement of resonant Raman and Rayleigh light scattering, an unusually broad J-band, and a non-zero extinction coefficient throughout the visible range. [33, 40, 41] In the present paper, we describe the formation of chiral J-aggregates of $TPPS_4$ under mildly acidic conditions in the presence of spermine, with added optically active tartrate as chiral inducer. We also wanted to consider an equally important and largely unexplored area of supramolecular chemistry, assembly degradation. Compared to aggregation, the reverse process

(disaggregation) has received little attention and it has been poorly described in the literature, thus far, for a very few examples. [42-49]

In particular, neither aggregate properties nor solution conditions under which disruption of the self-assembled structures occurs, have been outlined. Consequently, further research is required due to the importance that chemical modulation takes in the disassembling of such supramolecular systems and notably for the implications in the study of aggregation diseases. In the present case, the mesoscopic networks can be easily converted back to the monomeric state through the isolation of J-nanoaggregates building blocks by adding a highly charged polyanion, thus revealing chiroptical properties of meso and nano structures.

EXPERIMENTAL SECTION

The porphyrin meso-tetrakis(4sulfonatophenyl)porphyrin was purchased from Aldrich Co. as tetrasodium salt (≥ 98% pure). Aqueous concentrated solutions of the porphyrin ($1\text{-}2\times10^{-4}$ M) were prepared in dust-free Millipore water, stored in the dark and used within a day of preparation. Porphyrin solution concentrations were determined spectrophotometrically in water at neutral pH and zero ionic strength by using the value of the molar extinction coefficient at the Soret maximum (ε_{414} = $5.33\text{x}10^{5}$ M^{-1} cm^{-1}).[50] Poly(sodium vinylsulfonate) (PVS) was purchased from Sigma–Aldrich Co. (molecular weight ranging from 4000 up to 6000, 25% by weight). Polyelectrolyte concentration, expressed as moles of sulfonate units per liter, was obtained by weighing. Each polymer chain has a length of about 100 Å and supports about 38 sulfonate residues, which are approximately 2.5 Å apart from each other.[51] To avoid or minimize dust contamination, special care was taken by filtering all the

stock solutions through 0.22 μm Millipore filters. Spermine (1,12-diamino-4,9-diazadodecane) was purchased from Sigma. The pH values of the investigated samples were measured by using a Metrohm 744 pH meter (Metrohm, Herisau, Switzerland) by inserting a micro pH combined glass electrode. Samples of J-aggregated diacid $TPPS_4$ were prepared following a mixing protocol which involves the addition of a known volume of concentrated stock solution of spermine (100 μM) to a solution of porphyrin (3 μM) in 10 mM citrate or tartrate buffer at pH 3.2. In the case of disaggregation experiments promoted by the polymer and intended for the study of the effect of PVS load, in order to minimize any error, it was necessary to manage a starting J-aggregate system as reproducibly as possible. Taking advantage of the stability of the aggregated system within 24 hours of its preparation, we proceeded to its formation in special vials taking into account a suitable volume of reagents such as to allow an adequate number of disaggregation experiments (typically at least a dozen). Milli-Q water was used throughout.

RESULTS AND DISCUSSION

At pH 3.2 in tartrate buffer (10 mM) the UV/Vis spectra of $TPPS_4$ (3 μM) show the presence of the diprotonated monomeric porphyrin with a B-band at 434 nm (Figure 1a, dashed line). Under these mildly acidic conditions, $TPPS_4$ does not aggregate even after prolonged standing. However, upon addition of spermine (100 μM) evidence for extensive self-aggregation of the porphyrin is obtained: there is a marked decrease of the initial B-band concomitant with an increase of a new broad feature with maximum at 492 nm accompanied by a shoulder on its red-edge side (Figure 1a, red solid line). Although found at this same characteristic wavelength, this feature differs considerably from the usual

sharp band reported for $TPPS_4$ J-aggregates.[12] In addition, extinction throughout the entire visible range (to well above 800 nm) is observed. In Figure 1b the corresponding kinetic profiles for the $TPPS_4$/spermine aggregation are reported, exhibiting a sigmoidal behavior characterized by the presence of an initial induction period in the early stage, a profile very similar to that observed for the aggregation of $TPPS_4$ in strongly acidic aqueous solutions.[5] Previous investigations have shown that this type of profile is strongly affected by the mixing order of the reagents which influences the dynamics of growth and eventually both morphology and size of the assemblies.[32] A kinetic analysis of the extinction/time traces at 434 and 492 nm has been performed by using an autocatalytic model that assumes a rate determining step in which a *"critical size"* assembly forms, catalyzing further growth.[52] The rate constants for the uncatalyzed pathway, k_0, and for the catalyzed pathway, k_c, have relative values of about 1:15 and are in the range typical reported in the literature for similar processes.[53] Therefore, experimental data suggest as the autocatalytic pathway becomes more relevant compared to the parallel uncatalyzed process, being the former essentially promoted by the formation of germinal nuclei. The latter, with time, become even larger as monomers self-assemble so leading to the formation of highly reactive units. In this regard, the critical size for the nuclei, m, is between 5 and 6 interacting units and the time exponent n, that indicates the evolution of the fractal growth, is about 6. These findings are in line with previous results, suggesting as small oligomers in which the spermine acts as sticky agent, should be suitable as critical nuclei in the growth of J-aggregates.[32] The formation of mesoscopic aggregates in which porphyrins are electronically coupled causes an almost complete quenching of fluorescence emission and gives rise to a large enhancement of the resonant light scattering[54] at the red-edge of the extinction peak (Figure 1c). These aggregates are stable in

solution for a day or more after their preparation. The observed optical features are very similar to those obtained using citrate buffer at lower pH and they have been explained in terms of dipole-dipole (rather than Frenkel exciton) coupling among individual porphyrins belonging to the extended network formed by the J-aggregates and spermine.[40, 33] As expected for an achiral building block, when citrate is used as buffer, under the aforementioned experimental conditions, the obtained aggregates are <u>not</u> optically active as evidenced by silent circular dichroism spectra. In contrast, when L-tartrate buffer is used, quite strong bisignate CD signals having a positive Cotton effect are induced at 492 nm (J-band) and a somewhat weaker feature at 424 nm (H-band) is seen (Figure 1d). The CD spectra obtained for the enantiomeric D-tartrate are almost mirror images as expected.

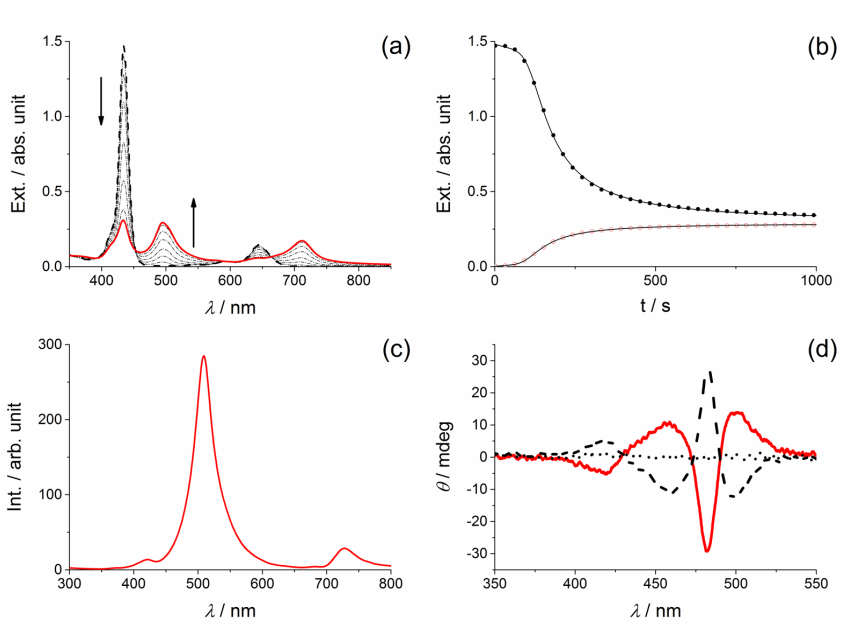

Figure 1. a) Extinction spectral changes for $TPPS_4$ J-aggregates induced by spermine (red solid line) starting from diacid monomeric porphyrin (dashed line); b) UV-vis corresponding kinetic profiles evaluated at λ = 434 (black full circles) and 492 nm (red open circles) (The kinetic analysis

according to eq. 1 gives: $k_0 = 4{,}6\times10^{-4}\pm5\times10^{-5}$; $k_c = 7{,}32\times10^{-3}\pm1\times10^{-5}$; m = 5.6±0.1; n = 6.4±0.2; R_2 = 0,99928); c) RLS spectrum feature recorded at the end of the aggregation process induced by spermine; d) Comparison among the CD spectra of the $TPPS_4$ aggregated solutions induced by L-tartrate (red solid line), D-tartrate (black dashed line) and citrate (black dotted line). Experimental conditions: [$TPPS_4$] = 3 μM; [Spermine] = 100 μM; 10 mM buffered solution at pH = 3.2; T = 298K.

According to our previously reported model for this supramolecular system,[32, 33, 40] nano-sized rod-like J-aggregates of the diacid $TPPS_4$ porphyrin are stabilized primarily via electrostatic interactions acting among adjacent porphyrins and involving the protonated cationic spermine. These nano-assemblies, together with porphyrin monomers, are embedded in a mesoscopic network in which spermine also plays an important role as bridging reagent. On the basis of this model, we thought it potentially enlightening to formulate a strategy to remove the cationic templating reagent and, thereby, disassemble the network. For this purpose we selected sodium poly(vinylsulfonate) (PVS), a highly negatively charged polyelectrolyte which has proven to be a very effective scavenger for positively charged polyamines. All these experiments were performed with fully formed, equilibrated spermine-induced porphyrin J-aggregates and a significant aspect of this study is how the efficiency of the process is related to the *"load"* of polymer employed. In the case of clusters obtained in the presence of D- or L-tartrate, below a polymer concentration value of 600 μM, nothing significant happens in terms of aggregate disruption, apart from an instantaneous large baseline upward shift exhibited in the extinction spectra (data not shown), followed by partial precipitation within a couple of hours. This behaviour is ascribable to the fact that, once the excess spermine, not involved in the

formation of the colloidal aggregate [40], has been neutralized by the polymer, the system undergoes charge neutralization, becoming unstable. An incipient disassembling of J-aggregates takes place above this concentration threshold, ranging between 600 and 900 μM (Figure S1, see SI). Extinction spectra show both a hypochromic effect in the aggregate region and a corresponding larger hyperchromic effect in the Soret region consistent with the restoration in solution of free diprotonated monomeric porphyrin. As evidenced by both kinetic profiles at 492 and 434 nm the disassembling process is quite slow. The temporal evolution of both circular dichroism (70% of hypochromicity) and resonance light scattering spectra (45% loss of intensity) are again consistent with the occurrence of porphyrin J-aggregates disassembling, a process that, under these experimental conditions, does not go to completion. Figure 2 shows an overview of the spectroscopic feature changes after the addition of about a 10-fold excess of PVS with respect to $TPPS_4$/spermine clusters obtained in the presence of L-tartrate. As expected, the disassembling process is faster than earlier as a consequence of increased PVS load. In the UV/Vis spectra (Figure 2a), initially the red-edge shoulder of the 492 nm band rapidly decreases leading to a previously undetected and unusual sharpening of this feature (more evident in the inset) and to a parallel increase of the absorbance at 434 nm, corresponding to the release of the diacid porphyrin. This step is afterwards followed by a slower disappearance of the 492 nm band and by the corresponding formation of fully monomeric diprotonated $TPPS_4$, a process that can be readily interpreted by the corresponding kinetic profiles reported in Figure 2b, which shows the aforementioned biphasic behavior. Indeed, a kinetic analysis of the spectral changes at 434 nm has been performed according to a biphasic pseudo-first order model, indicating that the release of the free monomer in solution occurs in an initial quite rapid step, followed by a slower one. The kinetic

rate constant for the first step is in good agreement with the kinetic evolution of extinction at 800 nm that can be described as a pseudo-first order process. On the other hand, the evolution of the extinction at 492 nm after an initial period showing minimal changes, evolves with pseudo-first order kinetics, whose observed rate constant matches closely the slower step detected at 434 nm. The disassembling of the porphyrin clusters is once again proved by resonance light scattering profiles from which, similar to what was observed in the extinction spectra, it is possible to distinguish biphasic behavior for the disappearance of the aggregated species (Figure 2c). More specifically, the addition of polymer leads the broad RLS feature (corresponding to porphyrin clusters) first to be gradually blue-shifted ($\Delta\lambda$=14 nm), then to a simultaneous and progressive narrowing and large increasing of the RLS intensity, reminiscent of porphyrin J-aggregates having a rod-like structure.[31] After the signal has reached a maximum intensity value, a slower decreasing of the RSL intensity follows until a set of spectral features are reached, consistent with the absence in solution of large porphyrin aggregates. The signal is only slightly larger than that of the neat solvent and shows a *"well"*, corresponding to the B-band due to photon loss due to absorption. The biphasic behavior of the kinetics fostered by PVS is shown in the inset of Figure 2c, where the time trace of RLS intensity collected at 496 nm closely resembles that observed in the extinction at 492 nm (on the J-band), reported in Figure 2b. A further confirmation of the disassembling process arises from the corresponding circular dichroism spectral changes. Soon after adding PVS, the broad positive component of the 492 nm J-band initially sharpens and slightly increases in intensity, due to the decrease of the differential scattering contribution.[55, 56] Subsequently, once again, all the bands in the CD spectra decrease in intensity, eventually approaching zero (Figure 2d). When D-tartrate is used as

buffer, all the general kinetic behavior fostered by PVS is similar to that observed with L-tartrate with respect to both intensity of signals and disassembly kinetic rates as showed in Figure S2 (see SI). When meso-tartrate buffer is used to prepare the J-aggregates, the final CD spectra of the clusters after complete aggregation are silent. Upon addition of an excess of PVS, a weak positive bisignate CD band develops corresponding to the intermediate formation of the nano-aggregates which eventually disappears (Figure S3a, see SI). On the other hand, the employment of DL-tartrate leads to a pattern similar to that of L-tartrate buffer but characterized by much weaker signals (Figure S3, see SI). These experimental findings allow us to propose a hypothetical mechanism for the assembling and disassembling process here investigated (Scheme 1).

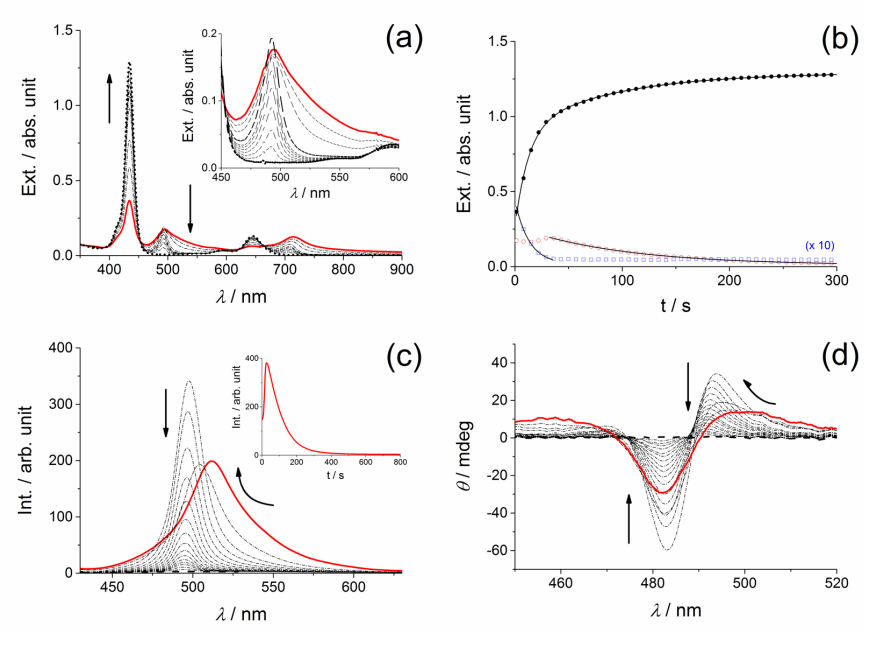

Figure 2. a) Extinction spectral changes for $TPPS_4$ J-aggregates (red solid line) disassembling process on adding PVS. The inset shows an enlarged portion of the extinction spectrum corresponding to the J-band feature; b) UV-vis corresponding kinetic profiles evaluated at λ = 434 (black full circles), 492

nm (red open circles) and 800 nm (blu full squares) (λ = 434 nm, k_{obs1} = 0.0945 ± 0.001 s^{-1}; k_{obs2} = 0.0118 ± 0.0001 s^{-1}, R^2= 0.9986. λ = 800 nm, k_{obs} = 0.100 ± 0.002 s^{-1}, R^2= 0.9869. λ = 492 nm, k_{obs} = 0.0086 ± 0.0001 s^{-1}, R^2= 0.9935); c) RLS spectral features changes for $TPPS_4$ J-aggregates (red solid line) on adding PVS. The inset shows the relative kinetic profile followed at 496 nm; d) CD spectral changes for $TPPS_4$ J-aggregates (red solid line) on adding PVS. Experimental conditions: [$TPPS_4$] = 3 μM; [Spermine] = 100 μM; [PVS] = 1100 μM; [L-Tartrate] = 10 mM buffered solution at pH = 3.2; T = 298K.

The diprotonated porphyrins self-assemble into small nano-arrays in which the basic interaction is the mutual electrostatic attraction between negatively charged sulfonate groups and positively charged pyrroles of adjacent macrocycle cores. Spermine is fully protonated at pH 3.2, a pH value fairly high with respect to that needed for porphyrin aggregation in the absence of a templating reagent, so it provides a pathway to lower the kinetic barrier for the approach of diprotonated $TPPS_4$ units that remain negatively charged at the periphery (Scheme 1, step 1 forward). The optically active tartrate anion provides a chiral bias to the oligomers. Once the initial chiral nuclei are formed, they constitute the building blocks for further aggregation processes leading to much larger clusters. These nano-clusters extend mainly by self-assembling of monomers onto the initial aggregates (Scheme 1, step 2 forward). This growth mechanism leads to a mesoscopic network [57] that, considering the low ionic strength conditions, is stabilized by the presence of the cationic polyamine. This latter acts either as an efficient capping reagent lowering the electrostatic repulsion, or by directly bridging different nano-

assemblies. In either case, the resulting clusters can still embed residual monomeric porphyrin due to the large excess of spermine. This hypothesis is supported by the occurrence of broad spectral features in the UV/Vis spectra, due to a dipole-dipole exciton coupling mechanism. [33, 57] Dynamic light scattering (DLS) measurements also confirm the presence in solution of micrometer-sized particles (1.42 ± 0.26 μm) with an intermediate, moderately polydisperse distribution size (0.38). The morphology of these aggregates has been obtained by scanning electron microscopy (SEM). Figure 3 shows the SEM image of a sample on a glass substrate from which the aforementioned mesoscopic network clearly appears as large sea urchin-like clusters with sizes spanning up to a few micrometers, constituted by smaller rod-like or nanotubular aggregates originating from common nuclei. These last findings achieved on glass surfaces agree with previous results obtained in solution by means of scattering techniques and focusing on the formation of micrometric objects having a fractal morphology and exhibiting highly peculiar optical properties. [33, 40] On adding the high density negatively charged-polymer (PVS) to these supramolecular structures, the experimental findings show a multiphasic process involving the following steps: i) an instantaneous electrostatic interaction between PVS and the tetracationic polyamine in excess not involved in the network (this step does not lead to any detectable spectral change); ii) an initial rapid removal of the positively charged spermine responsible for the stabilization of the mesoscopic network, thus releasing both free nano-assemblies and monomeric diprotonated $TPPS_4$ (Scheme 1, step 2 reverse); iii) a slower stripping out of the spermine involved in the electrostatic interactions inside the nano-assemblies (Scheme 1, step 1 reverse). The electrostatic interaction in the preliminary stage of re-verse step 2 is faster than the

mixing time being not detectable. On the other hand, the reverse step 2 is strictly dependent on polymer concentration being striking over a threshold value of 900 μM.

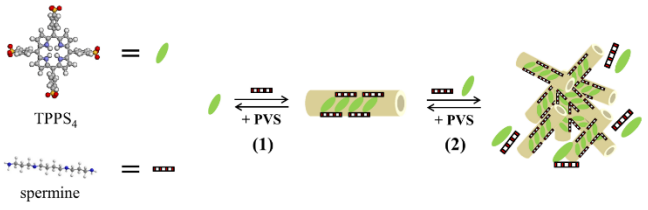

Scheme 1. Schematic model for J-aggregation of $TPPS_4$ induced by spermine and disassembling process promoted by poly(sodium vinylsulfonate).

This stage can be conveniently monitored through any of several spectroscopic techniques. It consists of a progressive blue shift and sharpening of the broad extinction feature, followed by a rapid increase of the J-band component. This latter achieves its maximum intensity in a time that is well matched with other experimental techniques. A further confirmation of the intrinsic nature of the mesoscopic disassembling process arises from the behaviour of the extinction kinetic profile followed at 800 nm (Figure 2b), a wavelength that does not match the absorption neither of the clusters, nor of the nano-assemblies. At this wavelength, the extinction is essentially ascribable to Rayleigh scattering contribution determined by the mesoscopic structure. The time evolution of this feature reaches a minimum intensity when the corresponding maximum of the J-band at 492 nm reaches its maximum intensity. This observation is an indirect proof that reverse step 2 is the disassembling of the mesoscopic structure into the basic nano-assemblies.

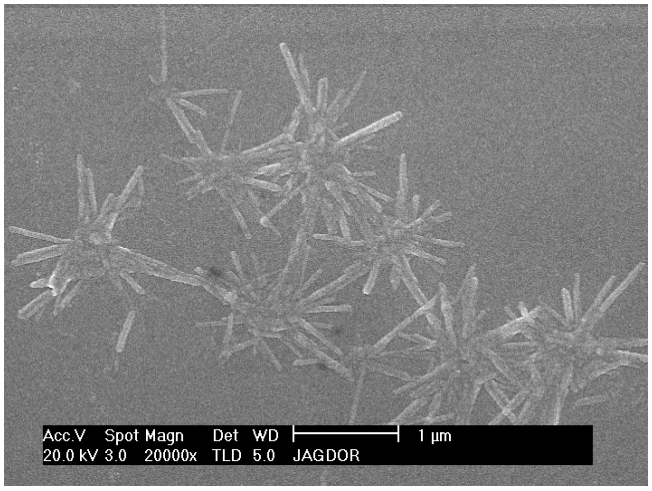

Figure 3 SEM image of clusters deposited on glass from aqueous solutions at pH 3.2 (T = 298 K, gold-coated).

As these latter structures are formed, they can be stabilized with respect to the subsequent disassembling step simply by adding a stoichiometric amount of additional spermine in order to neutralize the polymer load. Under these experimental conditions, the system is stable over time and the isolated 492 nm J-nanoaggregates have been characterized through DLS and SEM analysis. The former technique showed a monodisperse particle size distribution (0.12) with a corresponding particle diameter of 150 ± 5 nm. SEM revealed the presence of individual nano-objects spatially isolated on the surface with a size range spanning from approximately 100 to 300 nm (Figure 4). A residual amount of spermine covering the individual nano-objects is clearly detectable. In this framework, the reverse step 1 depicted in Scheme 1 is slowest, due mainly to the more difficult removal of the charged spermine that is intimately part of the structure of the nano-assemblies structure. The use of PVS aimed at the disassembling of $TPPS_4$/spermine clusters obtained in the presence of optically inactive citrate buffer (Figure S4, see SI), leads to some spectroscopic feature

changes identical to those observed in tartrate buffer. Nevertheless, the most striking aspect is the unexpected onset of chirality whereas the initial mesoscopic structure shows no induced circular dichroism signal. Figure 5 reports the temporal behaviour of CD spectra on adding PVS that show a quite strong bisignate CD signal having a positive Cotton effect induced at 492 nm (J-band). Its intensity decreases to zero in a time corresponding to complete disassembling, as observed via other spectroscopic techniques (Figure S4, see SI). The observation of induced CD signals appearing during the second stage of the disassembling process, confirms once again, the existence in solution of structures in which porphyrins are self-assembled in either a chiral rod-like or nanotube arrangement. These results are consistent with observations on the chiral induction of $TPPS_4$ J-aggregates in the absence of any chiral bias.[53] The observation of initially silent CD spectra for the J-aggregates obtained in the presence of citrate and the late manifestation of chirality during the disassembling process represents an intriguing problem. Nanorods and/or nanotubes are the basic building blocks for the mesoscopic aggregates. These species are chiral as evidenced by the intermediate CD spectra of the disassembling kinetics shown in Figure 5. Their spectra exhibit positive bisignate and slight asymmetric CD bands reminiscent of those reported for J-aggregates obtained under highly acidic conditions without the presence of any chiral inducer.[53]

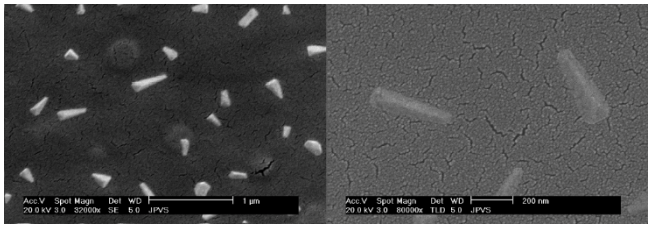

Figure 4 Low (left) and high (right) magnification SEM images of J-aggregates deposited on glass and obtained by disassembling the mesoscopic structure by means of poly(sodium vinylsulfonate). (T = 298 K, gold-coated).

The absence of CD signals for a mesoscopic structure obtained through a clustering of such chiral nanoaggregates could be explained by: *i)* a screening hypochromism mechanism, due to the interaction of the absorption dipole moment transitions; this mechanism has been invoked to explain the reduced extinction coefficient at the maximum of the absorption bands in molecular aggregates of a variety of chromophores, including porphyrins,[58] *ii)* the occurrence of differential scattering for these large structures; this effect could have a significant impact on the form and the intensity of the CD features, as reported for various biopolymers;[59] *iii)* a rearrangement of the nanoaggregates into chiral structures, following the removal of the excess spermine and the disruption of the mesoscopic aggregates and *iv)* an internal random arrangement of the nanoaggregates into the mesoscopic structures (see Figure 3), with a nulling effect due to geometrical factors.

Our evidence does not allow us to discriminate which of these is the operative mechanism or if there is an interplay among some of them. This issue is currently under investigation in our laboratories. At the moment, we consider mechanism *iii* less likely because it is already known that J-aggregates can give spontaneous symmetry breaking and display optical activity, even in the absence of chiral templating reagents. [53]

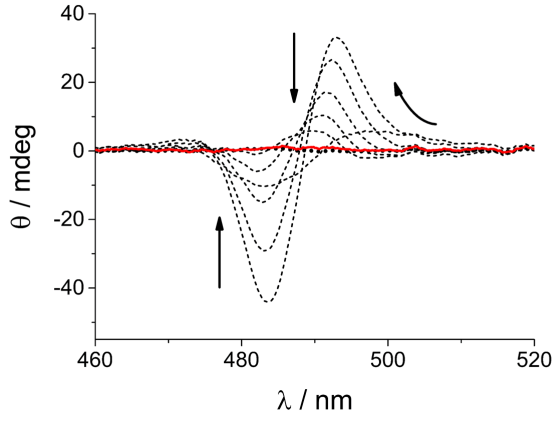

Figure 5 Circular dichroism spectral changes for $TPPS_4$ J aggregates (red solid line) on adding poly(sodium vinylsulfonate). Experimental conditions: [$TPPS_4$] = 3 μM; [Spermine] = 100 μM; [PVS] = 1100 μM; [Citrate] = 10 mM buffered solution at pH = 3.2; T = 298K.

As far as the CD signals detected for spermine induced J-aggregates in the presence of L or D tartaric buffer, the observation of initial broader and weaker bands that evolve into stronger and narrower spectral features could be due to the previously cited screening hypochromism mechanism. It is interesting to note that the sign of the bisignate CD bands is positive for L-tartrate buffer, mirrored by the spectral features of D-tartrate. These experimental findings are in agreement with what we previously reported for chiral fractal J-aggregates obtained in solution under higher ionic strength conditions (NaCl) to foster aggregation,[31] or when the aggregates form in the inner water pool of AOT microemulsions using the same enantiomers of tartaric acid.[34] With regard the point *iv* recently it has been reported as chiral multicromophoric fibers may provide a reversible disassemble into spherical structures with silent CD spectra by slightly increasing of the solvent polarity.[42]

CONCLUSIONS

In conclusion, spermine, a simple tetra-amine compound, is able to foster aggregation of the $TPPS_4$ porphyrin under mild acidic conditions, far different from the usual high ionic strength or acidic pH values normally required for such processes. The morphology of the resulting mesoscopic system is a consequence of the kinetics of growth. The tetracationic amine favors the self-assembly of diprotonated $TPPS_4$ units, leading to small nano-aggregates that eventually cluster through the involvement of an excess of spermine. Elongation and further growth of the nanoassemblies lead to the final sea urchin-like meso-structures. Dipole-dipole exciton coupling is responsible for the peculiar spectroscopic features of these supramolecular systems, including the strong enhancement of resonant light scattering and the general broadening of the UV/Vis spectra. These features are reminiscent of artificial light harvesting systems. The assembling and disassembling process, monitored through different spectroscopic techniques, is highly reproducible even in the presence of different acids. The presence of simple anionic chiral species (D or L-tartrate) in solution directs the chirality of the resulting aggregates. As already reported for closely related systems the chirality is expressed both at the nano- and at the meso-scale, being transferred from the chiral tartrate to the initial nano-aggregates and to the final clusters. More intriguing is the observation of chirality in the absence of any chiral templating reagents, that is once again related to the ongoing question of the apparent spontaneous symmetry breaking in $TPPS_4$ J-aggregates.[53]

Supporting Information. The following files are available free of charge.

Experimental Section, Extinction, RLS, CD Spectral changes and kinetic profiles for $TPPS_4$ J-aggregates disassembling process i) at different PVS load (S1-S2), ii) in presence of meso-tartrate and DL-tartrate (S3) and iii) citrate (S4).

AUTHOR INFORMATION

Corresponding Author

* Dr. Maria A. Castriciano CNR-ISMN, Istituto per lo Studio dei Materiali Nanostrutturati, c/o Dipartimento di Scienze Chimiche, Biologiche, Farmaceutiche ad Ambientali 98166, V.le F. Stagno D'Alcontres 31 Messina, Italy. E-mail: castriciano@pa.ismn.cnr.it

* Prof. Andrea Romeo Dipartimento di Scienze Chimiche, Biologiche, Farmaceutiche ad Ambientali, and C.I.R.C.M.S.B., University of Messina, V.le F. Stagno D'Alcontres 31, Vill. S. Agata, 98166 Messina, Italy. E-mail: anromeo@unime.it

Author Contributions

The manuscript was written through contributions of all authors. All authors have given approval to the final version of the manuscript.

Notes

In memory of Prof. Teodor Silviu Balaban.

ACKNOWLEDGMENT

The authors would like to thank Prof. R. F. Pasternack for helpful discussions and suggestions.

CNR and PRIN 2015 Prot. 2015XBZ5YA_004 for financial support.

REFERENCES

1. McHale, J. L., Hierarchal Light-Harvesting Aggregates and Their Potential for Solar Energy Applications. *J. Phys. Chem. Lett.* **2012,** *3*, 587-597.
2. Nam, Y. S.; Shin, T.; Park, H.; Magyar, A. P.; Choi, K.; Fantner, G.; Nelson, K. A.; Belcher, A. M., Virus-Templated Assembly of Porphyrins into Light-Harvesting Nanoantennae. *J. Am. Chem. Soc.* **2010,** *132*, 1462-1463.
3. Akins, D. L.; Zhu, H. R.; Guo, C., Absorption and Raman-Scattering by Aggregated Meso-Tetrakis(P-Sulfonatophenyl)Porphine. *J. Phys. Chem.* **1994,** *98*, 3612-3618.
4. Castriciano, M. A.; Romeo, A.; Villari, V.; Micali, N.; Scolaro, L. M., Nanosized Porphyrin J-Aggregates in Water/Aot/Decane Microemulsions. *J. Phys. Chem. B* **2004,** *108*, 9054-9059.
5. Castriciano, M. A.; Romeo, A.; Villari, V.; Micali, N.; Scolaro, L. M., Structural Rearrangements in 5,10,15,20-Tetrakis(4-Sulfonatophenyl)Porphyrin J-Aggregates under Strongly Acidic Conditions. *J. Phys. Chem. B* **2003,** *107*, 8765-8771.
6. Kano, H.; Kobayashi, T., Time-Resolved Fluorescence and Absorption Spectroscopies of Porphyrin J-Aggregates. *J. Chem. Phys.* **2002,** *116*, 184-195.
7. Koti, A. S. R.; Taneja, J.; Periasamy, N., Control of Coherence Length and Aggregate Size in the J-Aggregate of Porphyrin. *Chem. Phys. Lett.* **2003,** *375*, 171-176.
8. Maiti, N. C.; Mazumdar, S.; Periasamy, N., J- and H-Aggregates of Porphyrin-Surfactant Complexes: Time-Resolved Fluorescence and Other Spectroscopic Studies. *J. Phys. Chem. B* **1998,** *102*, 1528-1538.
9. Maiti, N. C.; Ravikanth, M.; Mazumdar, S.; Periasamy, N., Fluorescence Dynamics of Noncovalently Linked Porphyrin Dimers and Aggregates. *J. Phys. Chem.* **1995,** *99*, 17192-17197.
10. Micali, N.; Mallamace, F.; Romeo, A.; Purrello, R.; Scolaro, L. M., Mesoscopic Structure of Meso-Tetrakis(4-Sulfonatophenyl)Porphine J-Aggregates. *J. Phys. Chem. B* **2000,** *104*, 5897-5904.
11. Misawa, K.; Kobayashi, T., Ultrafast Exciton and Excited-Exciton Dynamics in J-Aggregates of Three-Level Porphyrin Molecules. *J. Chem. Phys.* **1999,** *110*, 5844-5850.
12. Ohno, O.; Kaizu, Y.; Kobayashi, H., J-Aggregate Formation of a Water-Soluble Porphyrin in Acidic Aqueous-Media. *J. Chem. Phys.* **1993,** *99*, 4128-4139.
13. Pasternack, R. F.; Schaefer, K. F.; Hambright, P., Resonance Light-Scattering-Studies of Porphyrin Diacid Aggregates. *Inorg. Chem.* **1994,** *33*, 2062-2065.
14. Purrello, R.; Scolaro, L. M.; Bellacchio, E.; Gurrieri, S.; Romeo, A., Chiral H- and J-Type Aggregates of Meso-Tetrakis(4-Sulfonatophenyl)Porphine on Alpha-Helical Polyglutamic Acid Induced by Cationic Porphyrins. *Inorg. Chem.* **1998,** *37*, 3647-3648.
15. Ribo, J. M.; Crusats, J.; Farrera, J. A.; Valero, M. L., Aggregation in Water Solutions of Tetrasodium Diprotonated Meso-Tetrakis(4-Sulfonatophenyl)Porphyrin. *J. Chem. Soc.-Chem. Commun.* **1994**, 681-682.

16. Rotomskis, R.; Augulis, R.; Snitka, V.; Valiokas, R.; Liedberg, B., Hierarchical Structure of Tpps4 J-Aggregates on Substrate Revealed by Atomic Force Microscopy. *J. Phys. Chem. B* **2004,** *108*, 2833-2838.
17. Schwab, A. D.; Smith, D. E.; Rich, C. S.; Young, E. R.; Smith, W. F.; de Paula, J. C., Porphyrin Nanorods. *J. Phys. Chem. B* **2003,** *107*, 11339-11345.
18. Würthner, F.; Kaiser, T. E.; Saha-Möller, C. R., J-Aggregates: From Serendipitous Discovery to Supramolecular Engineering of Functional Dye Materials. *Angew. Chem.-Int. Edit.* **2011,** *50*, 3376-3410.
19. Koti, A. S. R.; Periasamy, N., Self-Assembly of Template-Directed J-Aggregates of Porphyrin. *Chem. Mat.* **2003,** *15*, 369-371.
20. Randazzo, R.; Mammana, A.; D'Urso, A.; Lauceri, R.; Purrello, R., Reversible "Chiral Memory" in Ruthenium Tris(Phenanthroline)-Anionic Porphyrin Complexes. *Angew. Chem.-Int. Edit.* **2008,** *47*, 9879-9882.
21. Aquilanti, V.; Maciel, G. S., Observed Molecular Alignment in Gaseous Streams and Possible Chiral Effects in Vortices and in Surface Scattering. *Orig. Life Evol. Biosph.* **2006,** *36*, 435-441.
22. D'Urso, A.; Randazzo, R.; Lo Taro, L.; Purrello, R., Vortexes and Nanoscale Chirality. *Angew. Chem.-Int. Edit.* **2010,** *49*, 108-112.
23. Arteaga, O.; Canillas, A.; Crusats, J.; El-Hachemi, Z.; Llorens, J.; Sacristan, E.; Ribo, J. M., Emergence of Supramolecular Chirality by Flows. *ChemPhysChem* **2010,** *11*, 3511-3516.
24. Crusats, J.; El-Hachemi, Z.; Ribo, J. M., Hydrodynamic Effects on Chiral Induction. *Chem Soc Rev* **2010,** *39*, 569-577.
25. Escudero, C.; Crusats, J.; Diez-Perez, I.; El-Hachemi, Z.; Ribo, J. M., Folding and Hydrodynamic Forces in J-Aggregates of 5-Phenyl-10,15,20-Tris(4-Sulfophenyl)Porphyrin. *Angew. Chem.-Int. Edit.* **2006,** *45*, 8032-8035.
26. Ribo, J. M.; Crusats, J.; Sagues, F.; Claret, J.; Rubires, R., Chiral Sign Induction by Vortices During the Formation of Mesophases in Stirred Solutions. *Science* **2001,** *292*, 2063-2066.
27. Sorrenti, A.; El-Hachemi, Z.; Crusats, J.; Ribo, J. M., Effects of Flow-Selectivity on Self-Assembly and Auto-Organization Processes: An Example. *Chem. Commun.* **2011,** *47*, 8551-8553.
28. Micali, N.; Engelkamp, H.; van Rhee, P. G.; Christianen, P. C. M.; Scolaro, L. M.; Maan, J. C., Selection of Supramolecular Chirality by Application of Rotational and Magnetic Forces. *Nat. Chem.* **2012,** *4*, 201-207.
29. Mineo, P.; Villari, V.; Scamporrino, E.; Micali, N., Supramolecular Chirality Induced by a Weak Thermal Force. *Soft Matter* **2014,** *10*, 44-47.
30. Gandini, S. C. M.; Gelamo, E. L.; Itri, R.; Tabak, M., Small Angle X-Ray Scattering Study of Meso-Tetrakis (4-Sulfonatophenyl) Porphyrin in Aqueous Solution: A Self-Aggregation Model. *Biophys. J.* **2003,** *85*, 1259-1268.
31. Micali, N.; Villari, V.; Castriciano, M. A.; Romeo, A.; Scolaro, L. M., From Fractal to Nanorod Porphyrin J-Aggregates. Concentration-Induced Tuning of the Aggregate Size. *J. Phys. Chem. B* **2006,** *110*, 8289-8295.
32. Romeo, A.; Castriciano, M. A.; Scolaro, L. M., Spectroscopic and Kinetic Investigations on Porphyrin J-Aggregates Induced by Polyamines. *J. Porphyr. Phthalocyanines* **2010,** *14*, 713-721.

33. Scolaro, L. M.; Romeo, A.; Castriciano, M. A.; Micali, N., Unusual Optical Properties of Porphyrin Fractal J-Aggregates. *Chem. Commun.* **2005**, 3018-3020.
34. Castriciano, M. A.; Romeo, A.; De Luca, G.; Villari, V.; Scolaro, L. M.; Micali, N., Scaling the Chirality in Porphyrin J-Nanoaggregates. *J. Am. Chem. Soc.* **2011,** *133*, 765-767.
35. Claret, J.; Feliu, J. M.; Muller, C.; Ribo, J. M.; Serra, X., Reactivity of Pyrrole Pigments .6. Electrochemical Reduction of Some 5(1h)-Pyrromethenones and 5-Arylmethylene-3,4-Dimethyl-3-Pyrrolin-2-Ones. *Tetrahedron* **1985,** *41*, 1713-1720.
36. El-Hachemi, Z.; Balaban, T. S.; Campos, J. L.; Cespedes, S.; Crusats, J.; Escudero, C.; Kamma-Lorger, C. S.; Llorens, J.; Malfois, M.; Mitchell, G. R.; Tojeira, A. P.; Ribó, J. M., Effect of Hydrodynamic Forces on Meso-(4-Sulfonatophenyl)-Substituted Porphyrin J-Aggregate Nanoparticles: Elasticity, Plasticity and Breaking. *Chem Eur J* **2016**, *22*, 9740-9749.
37. Hollingsworth, J. V.; Richard, A. J.; Vicente, M. G. H.; Russo, P. S., Characterization of the Self-Assembly of Meso-Tetra(4-Sulfonatophenyl)Porphyrin ($H_2TPPS_4^-$) in Aqueous Solutions. *Biomacromolecules* **2011,** *13*, 60-72.
38. Short, J. M.; Berriman, J. A.; Kubel, C.; El-Hachemi, Z.; Naubron, J. V.; Balaban, T. S., Electron Cryo-Microscopy of Tpps4 Center Dot 2hcl Tubes Reveals a Helical Organisation Explaining the Origin of Their Chirality. *ChemPhysChem* **2013,** *14*, 3209-3214.
39. Wang, Z. C.; Medforth, C. J.; Shelnutt, J. A., Porphyrin Nanotubes by Ionic Self-Assembly. *J. Am. Chem. Soc.* **2004,** *126*, 15954-15955.
40. Micali, N.; Villari, V.; Scolaro, L. M.; Romeo, A.; Castriciano, M. A., Light Scattering Enhancement in an Aqueous Solution of Spermine-Induced Fractal J-Aggregate Composite. *Phys. Rev. E* **2005,** *72*, 4.
41. Villari, V.; Mazzaglia, A.; Trapani, M.; Castriciano, M. A.; de Luca, G.; Romeo, A.; Scolaro, L. M.; Micali, N., Optical Enhancement and Structural Properties of a Hybrid Organic-Inorganic Ternary Nanocomposite. *J. Phys. Chem. C* **2011,** *115*, 5435-5439.
42. Charalambidis, G.; Georgilis, E.; Panda, M. K.; Anson, C. E.; Powell, A. K.; Doyle, S.; Moss, D.; Jochum, T.; Horton, P. N.; Coles, S. J.; Linares, M.; Beljonne, D.; Naubron, J.-V.; Conradt, J.; Kalt, H.; Mitraki, A.; Coutsolelos, A. G.; Balaban, T. S., A Switchable Self-Assembling and Disassembling Chiral System Based on a Porphyrin-Substituted Phenylalanine–Phenylalanine Motif. *Nat Commun* **2016,** *7*, 12657.
43. Li, Y.; Steer, R. P., Kinetics of Disaggregation of a Non-Covalent Zinc Tetraphenylporphyrin Dimer in Solution. *Chem. Phys. Lett.* **2003,** *373*, 94-99.
44. Ma, H.; Wu, J.; Liang, W.; Chao, J., Study on the Association Phenomenon of Cyclodextrin to Porphyrin J-Aggregates by Nmr Spectroscopy. *J Incl Phenom Macrocycl Chem* **2007,** *58*, 221-226.
45. Occhiuto, I.; De Luca, G.; Trapani, M.; Scolaro, L. M.; Pasternack, R. F., Peripheral Stepwise Degradation of a Porphyrin J-Aggregate. *Inorg. Chem.* **2012,** *51*, 10074-10076.
46. Pasternack, R. F.; Gibbs, E. J.; Bruzewicz, D.; Stewart, D.; Engstrom, K. S., Kinetics of Disassembly of a DNA-Bound Porphyrin Supramolecular Array. *J. Am. Chem. Soc.* **2002,** *124*, 3533-3539.
47. Watanabe, K.; Kano, K., Time-Dependent Enzyme Activity Dominated by Dissociation of J-Aggregates Bound to Protein Surface. *Bioconjugate Chem* **2010,** *21*, 2332-2338.

48. Wu, J.-J.; Ma, H.-L.; Mao, H.-S.; Wang, Y.; Jin, W.-J., Investigation on Disassociation of Porphyrin J-Aggregates Induced by B-Cyclodextrins Using Absorption and Fluorescence Spectroscopy. *J. Photochem. Photobiol.* **2005,** *173*, 296-300.
49. Zhai, D.; Xu, W.; Zhang, L.; Chang, Y.-T., The Role of "Disaggregation" in Optical Probe Development. *Chem Soc Rev* **2014**, 43, 2402-2411.
50. Fleischer, E. B.; Palmer, J. M.; Srivastava, T. S.; Chatterjee, A., Thermodyamic and Kinetic Properties of an Iron-Porphyrin System. *J. Am. Chem. Soc.* **1971,** *93*, 3162-3167.
51. Castriciano, M. A.; Samperi, M.; Camiolo, S.; Romeo, A.; Monsù Scolaro, L., Unusual Stepwise Protonation and J-Aggregation of Meso-Tetrakis(N-Methylpyridinium-4-yl)Porphine on Binding Poly(Sodium Vinylsulfonate). *Chem Eur J* **2013,** *19*, 12161-12168.
52. Pasternack, R. F.; Gibbs, E. J.; Collings, P. J.; dePaula, J. C.; Turzo, L. C.; Terracina, A., A Nonconventional Approach to Supramolecular Formation Dynamics. The Kinetics of Assembly of DNA-Bound Porphyrins. *J. Am. Chem. Soc.* **1998,** *120*, 5873-5878.
53. Romeo, A.; Castriciano, M. A.; Occhiuto, I.; Zagami, R.; Pasternack, R. F.; Scolaro, L. M., Kinetic Control of Chirality in Porphyrin J-Aggregates. *J. Am. Chem. Soc.* **2014,** *136*, 40-43.
54. Pasternack, R. F.; Collings, P. J., Resonance Light-Scattering - a New Technique for Studying Chromophore Aggregation. *Science* **1995,** *269*, 935-939.
55. Bustamante, C.; Maestre, M. F.; Keller, D., Expressions for the Interpretation of Circular Intensity Differential Scattering of Chiral Aggregates. *Biopolymers* **1985,** *24*, 1595-1612.
56. Bustamante, C.; Tinoco, I.; Maestre, M. F., Circular Differential Scattering Can Be an Important Part of the Circular Dichroism of Macromolecules. *Proc. Natl. Acad. Sci. USA* **1983,** *80*, 3568-3572.
57. Micali, N.; Villari, V.; Romeo, A.; Castriciano, M. A.; Scolaro, L. M., Evidence of the Early Stage of Porphyrin Aggregation by Enhanced Raman Scattering and Fluorescence Spectroscopy. *Phys. Rev. E* **2007,** *76*, 6.
58. Vekshin, N. L., Screening Hypochromism in Molecular Aggregates and Biopolymers. *J. Biol. Phys.* **1999,** *25*, 339-354.
59. Bustamante, C.; Maestre, M. F.; Tinoco, I., Circular Intensity Differential Scattering of Light by Helical Structures. Ii. Applications. *J Chem Phys* **1980,** *73*, 6046-6055.

Graphical Abstract

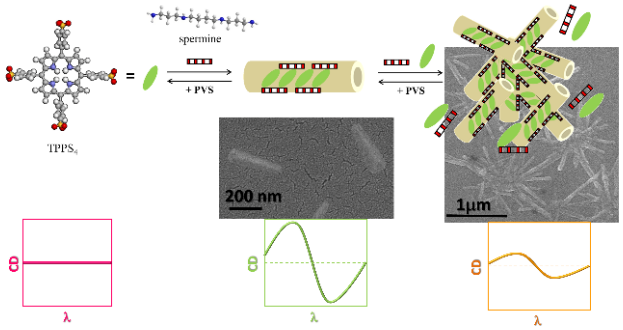

Electronic Supporting Information

for

Tuning supramolecular chirality in nano and mesoscopic porphyrin J-aggregates

Roberto Zagami,[‡] Maria A. Castriciano,[‡] Andrea Romeo,[‡,†] * Mariachiara Trapani,[‡] Rolando Pedicini,[#] Luigi Monsù Scolaro[‡,†].*

[‡] CNR-ISMN, Istituto per lo Studio dei Materiali Nanostrutturati, c/o Dipartimento di Scienze Chimiche, Biologiche, Farmaceutiche ad Ambientali 98166, V.le F. Stagno D'Alcontres 31 Messina, Italy. E-mail: castriciano@pa.ismn.cnr.it

[†] Dipartimento di Scienze Chimiche, Biologiche, Farmaceutiche ad Ambientali, and C.I.R.C.M.S.B., University of Messina, V.le F. Stagno D'Alcontres 31, Vill. S. Agata, 98166 Messina, Italy. E-mail: anromeo@unime.it

[#] CNR-ITAE Istituto di Tecnologie Avanzate per l'Energia, Via Salita Santa Lucia Sopra Contesse 5, 98126, Messina, Italy

Table of Contents

1 Experimental

p.3

1.1 Instruments

p.3

Extinction, RLS, CD spectral changes and kinetic profiles for $TPPS_4$ J-aggregates disassembling process on adding a low load of PVS (Fig. S1)

p.4

Extinction, RLS, CD Spectral changes and kinetic profiles for $TPPS_4$ J-aggregates disassembling process on adding a high load of PVS (Fig. S2)

p.5

CD spectral changes for $TPPS_4$ J-aggregates on adding PVS in presence of meso-tartrate and DL-tartrate (Fig. S3)

p.6

Extinction, RLS, CD Spectral changes and kinetic profiles for $TPPS_4$ J-aggregates disassembling process on adding PVS in presence of citrate (Fig. S4)

p.7

1.1 Instruments

UV/Vis spectra were obtained on a Hewlett–Packard 8453 diode array spectrophotometer using 1 cm pathlength quartz cells. Fluorescence emission and resonance light scattering (RLS) experiments were performed on a Jasco model FP-750 spectrofluorometer equipped with a Hamamatsu R928 photomultiplier, adopting for RLS experiments a synchronous scan protocol with right angle geometry [1]. RLS spectra were not corrected for the absorption of the samples. The circular dichroism (CD) spectra were recorded on a JASCO J-720 spectropolarimeter, equipped with a 450 W xenon lamp. The ellipticity was obtained by calibrating the instrument with a 0.06% aqueous solution of R-camphorsulfonic acid. CD spectra were corrected both for the cell and solvent contributions. SEM images were obtained by using a field emission Scanning Electron Microscope (Philips mod. XL30 SFEG). A colloidal graphite aqueous base (TAAB) was used to fix samples on the stab. Additionally, in order to make them electrically active, they were coated with gold. Hydrodynamic particle sizes and size distributions were measured by dynamic light scattering (DLS) and carried out at 25°C by a Zetasizer Nano-ZS (Malvern Instruments) equipped with a 633 nm He–Ne laser using backscattering detection. Each DLS sample was measured several times, and the results were averaged. The kinetic analyses of the extinction profiles have been achieved through a non-linear fit of the data according equation 1:

$$(Ext = Ext_\infty + (Ext_0 - Ext_\infty)\,(1 + (m - 1)\{k_0 t + (n + 1)^{-1}\,(k_c\,t)^{n+1}\})^{-1/(m-1)} \qquad (1)$$

(Ext, Ext_0 and Ext_∞ are the extinction at time t, at starting time and at the end of aggregation, respectively) [2].

[1] R. F. Pasternack and P. J. Collings, *Science* **1995**, *269*, 935-939.
[2] R. F. Pasternack, E. J. Gibbs, P. J. Collings, J. C. dePaula, L. C. Turzo and A. Terracina, *J. Am. Chem. Soc.* **1998**, *120*, 5873-5878.

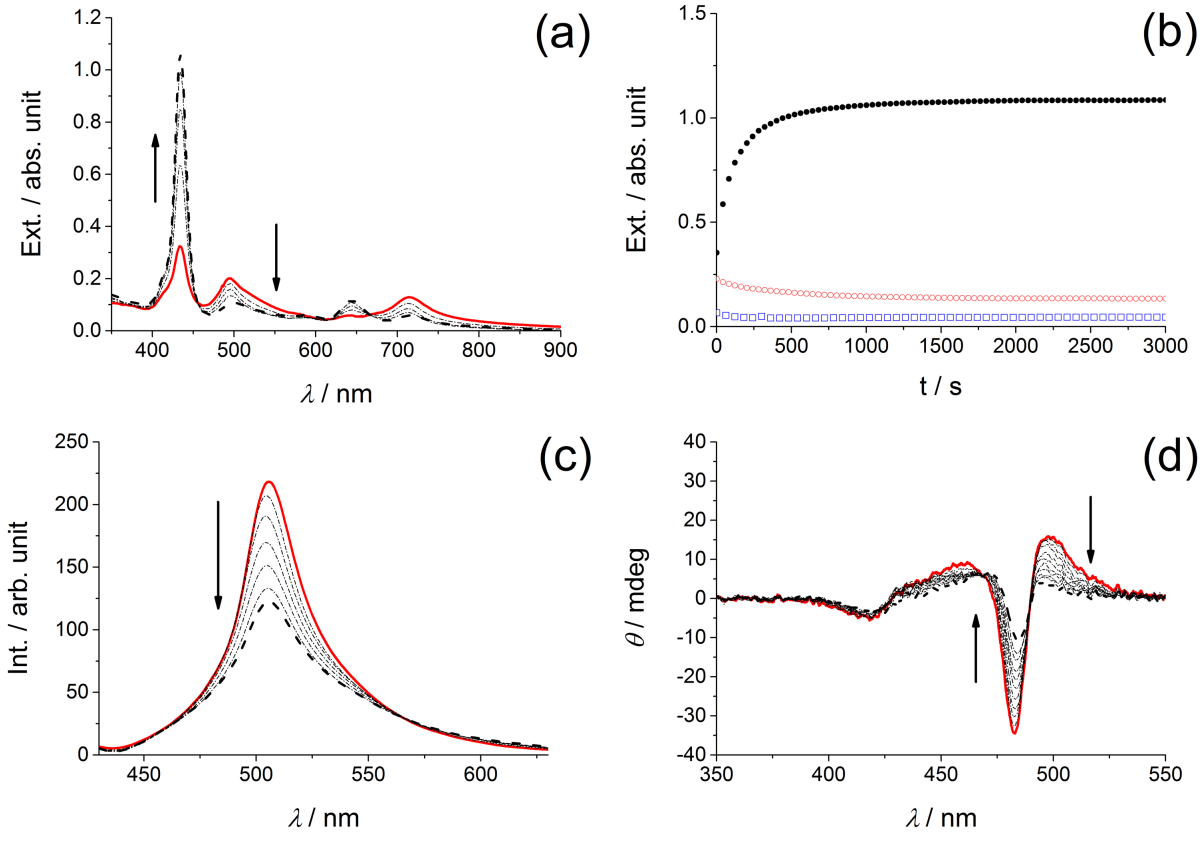

Figure S1 a) Extinction spectral changes for $TPPS_4$ J-aggregates (red solid line) disassembling process on adding PVS; b) UV-vis corresponding kinetic profiles evaluated at λ = 434 (black full circles), 492 nm (red open circles) and 800 nm (blu full squares); c) RLS spectral features changes for $TPPS_4$ J-aggregates (red solid line) on adding PVS; d) CD spectral changes for $TPPS_4$ J-aggregates (red solid line) on adding PVS. Experimental conditions: [$TPPS_4$] = 3 μM; [Spermine] = 100 μM; [PVS] = 700 μM; [L-Tartrate] = 10 mM buffered solution at pH = 3.2; T = 298K.

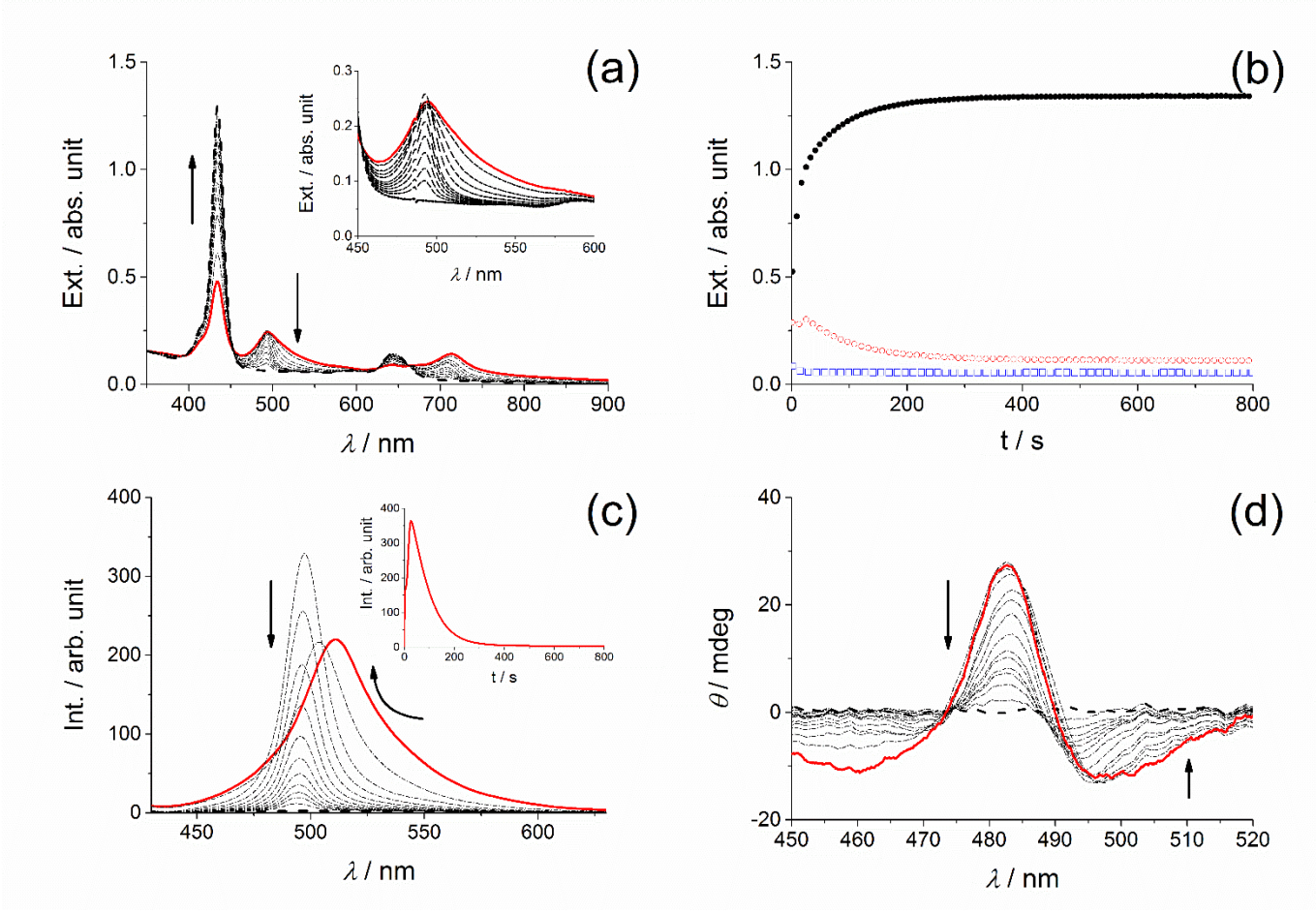

Figure S2 a) Extinction spectral changes for $TPPS_4$ J-aggregates (red solid line) disassembling process on adding PVS. The inset shows an enlarged portion of the extinction spectrum corresponding to the J-band feature; b) UV-vis corresponding kinetic profiles evaluated at λ = 434 (black full circles), 492 nm (red open circles) and 800 nm (blu full squares); c) RLS spectral features changes for $TPPS_4$ J-aggregates (red solid line) on adding PVS. The inset shows the relative kinetic profile followed at 496 nm; d) CD spectral changes for TPPS4 J-aggregates (red solid line) on adding PVS. Experimental conditions: [$TPPS_4$] = 3 μM; [Spermine] = 100 μM; [PVS] = 1100 μM; [D-Tartrate] = 10 mM buffered solution at pH = 3.2; T = 298K.

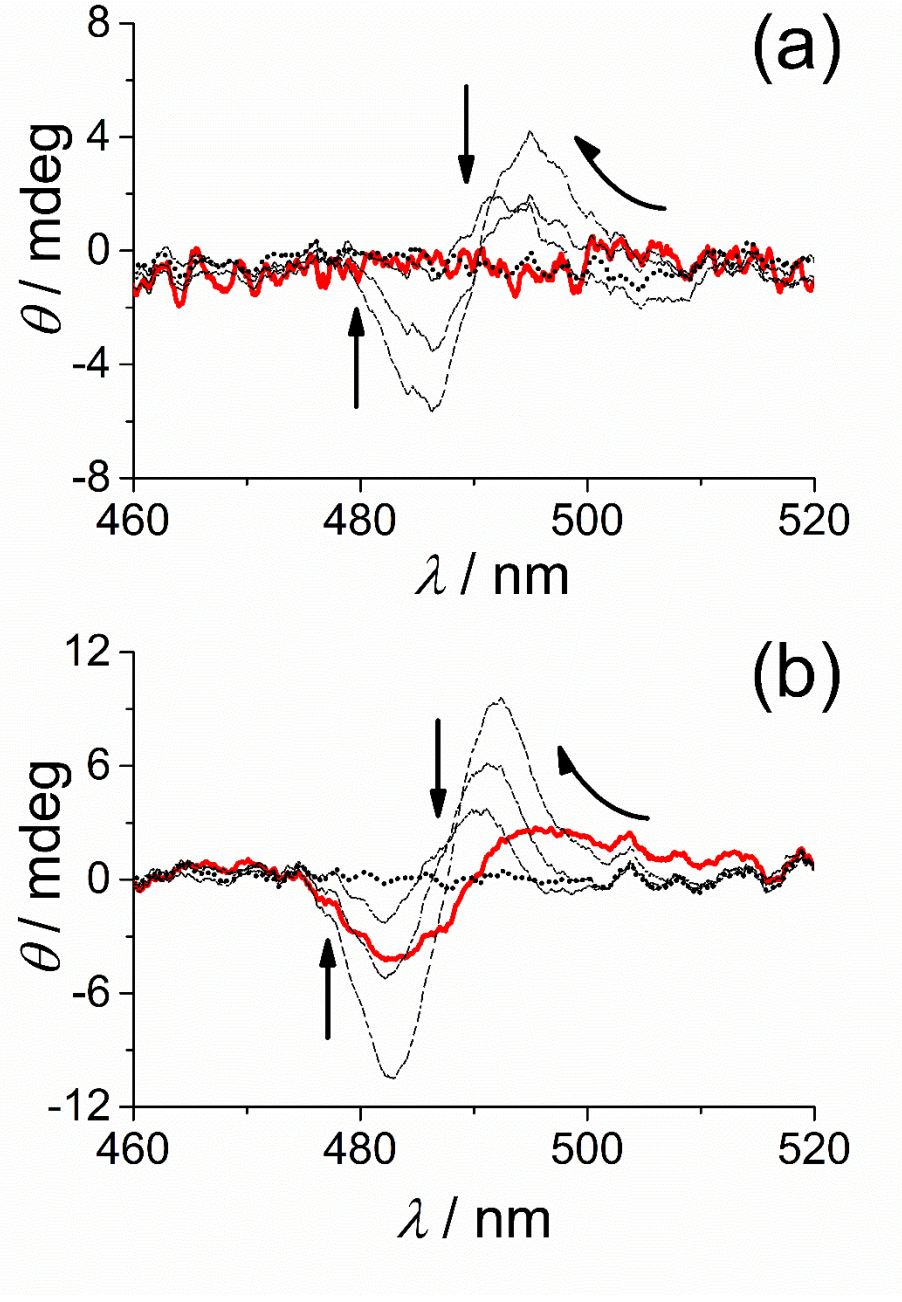

Figure S3 Circular dichroism spectral changes for $TPPS_4$ J-aggregates on adding PVS in presence of meso-tartrate (a) and DL-tartrate (b) being the red solid lines corresponding to the spectra recorded at the end of the aggregation process. Experimental conditions: [$TPPS_4$] = 3 μM; [Spermine] = 100 μM; [PVS] = 1100 μM; [Tartrate] = 10 mM buffered solution at pH = 3.2; T = 298K.

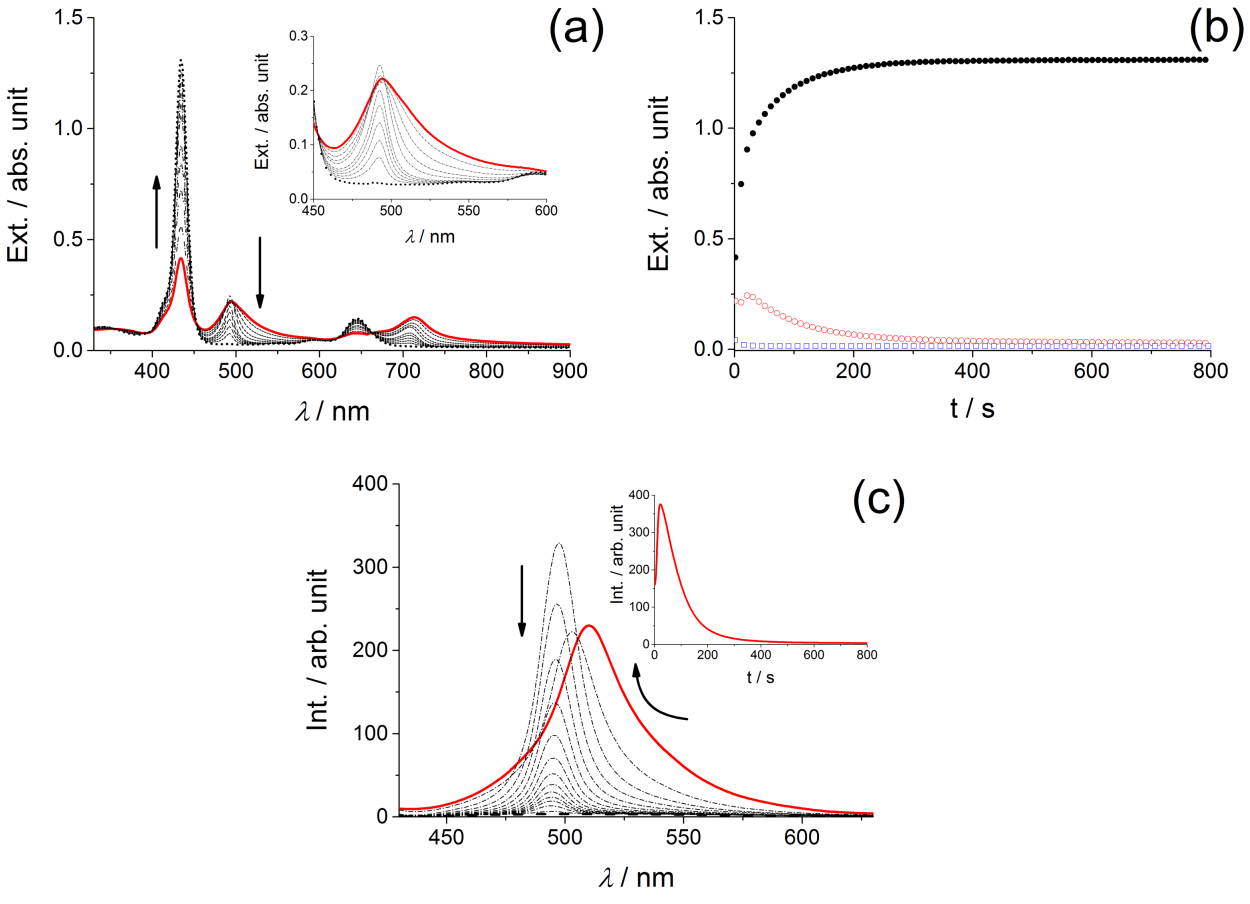

Figure S4 a) Extinction spectral changes for $TPPS_4$ J-aggregates (red solid line) disassembling process on adding PVS. The inset shows an enlarged portion of the extinction spectrum corresponding to the J-band feature; b) UV-vis corresponding kinetic profiles evaluated at λ = 434 (black full circles), 492 nm (red open circles) and 800 nm (blu full squares); c) RLS spectral features changes for TPPS4 J-aggregates (red solid line) on adding PVS. The inset shows the relative kinetic profile followed at 496 nm. Experimental conditions: [TPPS4] = 3 μM; [Spermine] = 100 μM; [PVS] = 1100 μM; [Citrate] = 10 mM buffered solution at pH = 3.2; T = 298K.